

# Steady-state kinetics of the NO–CO reaction on Rh(111): extrapolation from $10^{-10}$ to 1 bar

V.P. Zhdanov<sup>a,b,1</sup> and B. Kasemo<sup>a</sup>

<sup>a</sup>*Department of Applied Physics, Chalmers University of Technology, S-412 96 Göteborg, Sweden and*

<sup>b</sup>*Institute of Catalysis, Novosibirsk 630090, Russia*

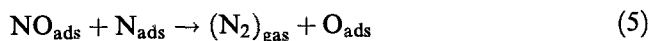
Received 30 January 1996; accepted 23 April 1996

Ultrahigh vacuum studies indicate that the mechanism of the NO–CO reaction on Rh(111) involves reversible adsorption of NO and CO, NO decomposition, nitrogen desorption, and a Langmuir–Hinshelwood reaction between CO and oxygen. Employing available experimental data for the rate constants of these steps, we have calculated the steady-state reaction kinetics in a wide range of pressures and temperatures. At relatively high pressures ( $P_{\text{NO}} \approx P_{\text{CO}} \approx 0.01$  bar), the results of simulations are in marginal agreement with the experimental data. Analyzing the difference between the theory and experiment makes it possible to understand the type of changes which might be introduced into the model in order to improve the agreement with the experiment.

**Keywords:** “pressure-gap” problem; reaction mechanism; elementary steps; rate constants; lateral interactions

One of the motivations of the development of surface science is connected with expectations that the kinetic data obtained at ultrahigh vacuum (UHV) can be extrapolated to practical conditions. During the past decade, there have been a few attempts to make such extrapolations. The available examples include ammonia synthesis on Fe [1], NO–CO reaction on Rh [2,3], CO oxidation on Rh [2] and Pt [4], hydrogen oxidation on Pt [5], water–gas shift reaction on Cu [6] and methanol synthesis on Cu [7].

Among the treatments mentioned above, the analysis of the NO–CO reaction on Rh(111), which is the present subject, given by Oh et al. [2] was considered to be very successful (see, e.g., a review by Taylor [8]). The mechanism of this reaction, based primarily on the results of the temperature-programmed desorption (TPD) measurements, was assumed to be as follows:



Employing for these steps the rate constants obtained from UHV surface chemistry studies, Oh et al. have

quantitatively described the steady-state reaction kinetics at temperatures and pressures interesting from the practical point of view ( $T = 400\text{--}700$  K and  $P_{\text{NO}} \approx P_{\text{CO}} \approx 0.01$  bar). The simulations carried out indicated that the Rh(111) surface is predominately covered with nitrogen atoms (e.g.,  $\theta_{\text{N}} = 0.96$  and  $0.99$  at  $P_{\text{NO}} = P_{\text{CO}} = 0.01$  bar and  $T = 500$  and  $675$  K, respectively), i.e., the nitrogen desorption is a rate-limiting step. Nitrogen atom removal was expected to occur primarily via step (4) or (5) at relatively high or low temperatures, respectively.

New experimental data on the NO–CO reaction on Rh(111) obtained during the nineties have shown that the model employed by Oh et al. [2] needs to be revised. The two key findings are connected with  $\text{N}_2\text{O}$  production [9–12] and nitrogen desorption [13,14].

At UHV conditions,  $\text{N}_2\text{O}$  formation is lacking on Rh(111) both in TPD and steady-state regimes (refs. [15,16] and ref. [17], respectively). At relatively high pressures (about 0.01 bar),  $\text{N}_2\text{O}$  production on Rh(111) was assumed to be negligible as well and was not directly monitored [2,18]. For supported Rh catalysts, this channel is known to be important at low temperatures and low conversions (just around and after light-off), whereas  $\text{N}_2$  formation dominates at higher temperatures [8,19]. Belton et al. [9–12] reexamined the NO–CO reaction on Rh(111) at relatively high pressures and found that the rate of  $\text{N}_2\text{O}$  formation can be comparable with that for  $\text{N}_2$ , just as for supported Rh. Another important conclusion from their studies is that dissociative readsorption of gas-phase  $\text{N}_2\text{O}$  does not seem to be efficient enough on Rh(111) to produce significant amount of  $\text{N}_2$  [11] (a reaction scheme including readsorption of  $\text{N}_2\text{O}$  has been analyzed by Cho [3]).

Recombination of nitrogen atoms on Rh is usually

<sup>1</sup> To whom correspondence should be addressed.

explored by employing TPD [15,16]. In such experiments, nitrogen is produced via NO adsorption and decomposition. If NO decomposition occurs thermally in the course of TPD, it is accompanied by NO desorption. In the framework of this scheme, one cannot obtain nitrogen coverages above 0.25 ML (1 ML corresponds to  $1.6 \times 10^{15}$  atoms per  $\text{cm}^2$ ). In addition, the kinetics of  $\text{N}_2$  desorption is affected by the presence of oxygen on the surface. To overcome these shortcomings, one needs to employ non-standard ways of nitrogen adsorption. Experiments of the latter type have been done by Bugyi and Solymosi [13] and Belton et al. [14]. To form the nitrogen overlayer, the former group used atomic nitrogen generated in a high-frequency discharge tube. The latter one employed electron beam dissociation of adsorbed NO (oxygen was cleaned off via the  $\text{O} + \text{CO}$  reaction). The results obtained indicate that at appreciable coverages the rate of nitrogen desorption is high already at relatively low temperatures (slightly above 400 K). This finding in turn changes an interpretation of the NO TPD spectra. In particular, one can conclude that the low-temperature  $\text{N}_2$  TPD peak, observed during NO decomposition on Rh(111) and attributed in the past to step (5) [2,15], is rather connected with nitrogen associative desorption (step (4)).

Simulations of associative desorption of N atoms from the Rh(111) surface in the framework of the lattice-gas model [20] make it possible to compare the  $\text{N}_2$  desorption rate calculated at different coverages with that measured during NO decomposition on Rh(111) at steady-state conditions. At temperatures and pressures interesting from a practical point of view, the measured rate is of the same order of magnitude as the calculated one if the coverage of nitrogen atoms is about 0.45. Thus, the steady-state nitrogen coverage cannot be as high as that predicted by Oh et al. [2]. The analysis of the kinetics of the NO–CO reaction on Rh presented by Cho [3] and explicitly based on the assumption that the  $\text{N}_2$  desorption rate (step (4)) is negligible compared to the rate of  $\text{N}_2$  formation via other steps also does not appear to be correct.

In the present communication, we outline briefly the results of our analysis of the kinetics of the NO–CO reaction on Rh(111) (a complete version of the paper will be published elsewhere [21]). The mechanism we employ is basically the same as that used by Oh et al. [2]. The only difference is that, referring to the  $\text{N}_2$  TPD data [13,14], we ignore step (5).  $\text{N}_2\text{O}$  formation is ignored as well (like in ref. [2]). The latter is reasonable at UHV conditions [15–17]. At relatively high pressures, the rates of  $\text{N}_2$  and  $\text{N}_2\text{O}$  formation may be comparable at some temperatures, but both rates are much lower compared to the adsorption/desorption rates of NO and CO. Under such circumstances, one may assume that the  $\text{N}_2$ - and  $\text{N}_2\text{O}$ -formation channels operate in parallel and almost independently. Thus, the second channel is not expected to perturb the first one considerably. In other words, the

$\text{N}_2\text{O}$ -formation channel can just be added if desired. Taking into account all these points and also that the mechanism and rate constants for  $\text{N}_2\text{O}$  formation are in fact lacking at present, it seems to be justifiable to omit this step in the simulations.

Assuming the adsorbed overlayer to be uniform (avoiding this approximation is not straightforward at present), we employ the following kinetic equations for describing steps (1)–(4) and (6):

$$d\theta_{\text{NO}}/dt = k_{\text{NO}}^{\text{ads}} P_{\text{NO}} \theta_v - k_{\text{NO}}^{\text{des}} \theta_{\text{NO}} - k_{\text{dec}} \theta_{\text{NO}} \theta_v, \quad (7)$$

$$d\theta_{\text{CO}}/dt = k_{\text{CO}}^{\text{ads}} P_{\text{CO}} \theta_v - k_{\text{CO}}^{\text{des}} \theta_{\text{CO}} - k_r \theta_{\text{CO}} \theta_{\text{O}}, \quad (8)$$

$$d\theta_{\text{N}}/dt = k_{\text{dec}} \theta_{\text{NO}} \theta_v - k_{\text{N}_2}^{\text{des}} \theta_{\text{N}}^2, \quad (9)$$

$$d\theta_{\text{O}}/dt = k_{\text{dec}} \theta_{\text{NO}} \theta_v - k_r \theta_{\text{CO}} \theta_{\text{O}}, \quad (10)$$

where  $k_{\text{NO}}^{\text{ads}}$ ,  $k_{\text{NO}}^{\text{des}}$ ,  $k_{\text{dec}}$  and  $k_r$  are the rate constants for NO and CO adsorption and desorption, NO decomposition and CO oxidation, respectively,  $\theta_{\text{tot}} = \theta_{\text{NO}} + \theta_{\text{CO}} + \theta_{\text{N}} + \theta_{\text{O}}$  is the total coverage,  $\theta_v = 1 - \theta_{\text{tot}}/\theta_s$  is the fraction of vacant sites, and  $\theta_s = 0.8$  is the saturation coverage which is assumed to be the same for all the particles ( $\theta = 1$  corresponds to 1 ML).

Analyzing TPD data for steps (1)–(4) and (6) [20–22], we conclude that the rate constants  $k_{\text{N}_2}^{\text{des}}$ ,  $k_{\text{CO}}^{\text{des}}$ ,  $k_{\text{NO}}^{\text{des}}$ ,  $k_{\text{dec}}$  and  $k_r$  are strongly dependent on coverage, and this dependence is an essential ingredient of simulations of the reaction kinetics both at low and high pressures. For such steps as CO or  $\text{N}_2$  desorption, the dependence of the desorption rate constants on CO and N coverages can be described in detail in the framework of the quasi-chemical or Bethe–Peierls approximations taking into account nearest-neighbour adsorbate–adsorbate lateral interactions [20,21]. For the whole reaction, the detailed analysis is hardly possible and we are enforced to limit ourselves by employing the simplest mean-field approximation (as it is described in ref. [23]). The input data for this approximation are the pre-exponential factors, activation energies at low coverages, and nearest-neighbour interactions in the ground and activated states (the terms “ground” and “activated” correspond in our context to the language of the transition state theory (TST)). In our simulations, we use the pre-exponential factors predicted by TST (table 1). All the activation energies corresponding to low coverages were obtained from TPD data (as discussed in detail in ref. [21]). The adsorbate–adsorbate interactions were also estimated (where possible) from TPD.

Our analysis of the CO,  $\text{N}_2$  and NO TPD spectra indicate that the CO–CO lateral interaction in the ground state is in fact nearly the same as the N–N interaction,  $\epsilon_{\text{CO–CO}} \approx \epsilon_{\text{N–N}} = 1.7$  kcal/mol [20,21], and that  $\epsilon_{\text{NO–NO}} \approx \epsilon_{\text{NO–N}} \approx \epsilon_{\text{NO–O}}$  [22]. The lateral interactions in the activated state for desorption are negligible. Using these and some other data [21], we approximate the cov-

Table 1

Kinetic parameters for the NO–CO reaction on Rh(111):  $\mathcal{K}$  are the rate constants for the reactant fluxes,  $s$  the sticking coefficients,  $\nu$  the pre-exponential factors, and  $E$  the activation energies

CO adsorption:	$k_{\text{CO}}^{\text{ads}} = s(0)\mathcal{K}, s(0)=0.8, \mathcal{K} = 1.8 \times 10^8 (300/T)^{1/2} \text{ s}^{-1} \text{ bar}^{-1}$
CO desorption:	$k_{\text{CO}}^{\text{des}}, \nu_{\text{des}} = 10^{16} \text{ s}^{-1}, E_{\text{des}}^0 = 38 \text{ kcal/mol}$
NO adsorption:	$k_{\text{NO}}^{\text{ads}} = s(0)\mathcal{K}, s(0)=0.8, \mathcal{K} = 1.7 \times 10^8 (300/T)^{1/2} \text{ s}^{-1} \text{ bar}^{-1}$
NO desorption:	$k_{\text{NO}}^{\text{des}}, \nu_{\text{des}} = 10^{16} \text{ s}^{-1}, E_{\text{des}}^s = 34 \text{ kcal/mol}$
nitrogen desorption:	$k_{\text{N}_2}^{\text{des}}, \nu_{\text{d}} = 10^{13} \text{ s}^{-1}, E_{\text{des}}^0 = 44 \text{ kcal/mol}$
NO decomposition:	$k_{\text{NO}}^{\text{dec}}, \nu_{\text{dec}} = 10^{13} \text{ s}^{-1}, E_{\text{dec}}^0 = 19 \text{ kcal/mol}$
CO+O reaction:	$k_{\text{r}}, \nu_{\text{r}} = 10^{13} \text{ s}^{-1}, E_{\text{r}}^0 = 26 \text{ kcal/mol}$
lateral interactions (in kcal/mol):	$\epsilon_1 = 1.7, \epsilon_2 = 1.0, \epsilon_{\text{eff}} = 7/6, \epsilon_1^* = 0.7$
number of nearest-neighbour sites:	$z = 6$
density of sites:	$N_0 = 1.6 \times 10^{15} \text{ cm}^{-2}$

erage dependence of the activation energies for CO, N<sub>2</sub> and NO desorption as

$$\text{CO: } E_{\text{des}} = E_{\text{des}}^0 - z\epsilon_1(\theta_{\text{CO}} + \theta_{\text{O}} + \theta_{\text{N}}) - z\epsilon_2\theta_{\text{NO}}, \quad (11)$$

$$\text{N}_2: E_{\text{des}} = E_{\text{des}}^0 - 2(z-1)\epsilon_1(\theta_{\text{CO}} + \theta_{\text{O}} + \theta_{\text{N}}) - 2(z-1)\epsilon_2\theta_{\text{NO}}, \quad (12)$$

$$\text{NO: } E_{\text{des}} = E_{\text{des}}^s - z\epsilon_2(\theta_{\text{tot}} - \theta_{\text{s}}), \quad (13)$$

where  $\epsilon_1 = 1.7 \text{ kcal/mol}$  is the nearest-neighbour interaction typical for CO and N,  $\epsilon_2$  is the nearest-neighbour interaction typical for NO,  $z = 6$  is the number of nearest-neighbour sites, and  $E_{\text{des}}^0$  and  $E_{\text{des}}^s$  are the activation energies for desorption at low coverages and near saturation, respectively (for NO, we prefer to use  $E_{\text{des}}^s$  instead of  $E_{\text{des}}^0$  because the former value can be obtained directly from the experiment). The value of the interaction  $\epsilon_2$  is lacking.

Decomposition of an adsorbed NO molecule is possible provided that it has an empty nearest-neighbour site for the oxygen (or nitrogen) dissociation product. For this reason, the NO decomposition rate is assumed to be proportional to  $\theta_{\text{v}}$ . This factor alone is however not sufficient in order to describe correctly the coverage dependence of the decomposition rate because in analogy with other elementary steps the process under consideration can also be affected by adsorbate–adsorbate interaction (for a general discussion, see ref. [24]). The experiment indicates that at relatively low coverages the rate constant  $k_{\text{dec}}$  rapidly decreases with increasing coverage [16]. Data for high coverages are unfortunately not available. In our calculations, we assume that

$$E_{\text{dec}} = E_{\text{dec}}^0 + z\epsilon_{\text{eff}}\theta_{\text{tot}}, \quad (14)$$

where  $\epsilon_{\text{eff}}$  is the effective lateral interaction, taking into account the interactions in the ground and activated states.

Detailed data on the coverage dependence of the activation energy for CO oxidation are not too important for our analysis because this step is fairly rapid. In our simulations, we employ the following dependence [21]:

$$E_{\text{r}} = E_{\text{r}}^0 + 2(z-1)(\epsilon_1^* - \epsilon_1)\theta_{\text{tot}}, \quad (15)$$

where  $\epsilon_1^* = 0.7 \text{ kcal/mol}$  is the interaction in the activated state.

In the kinetic model described, we have in fact two free parameters,  $\epsilon_2$  and  $\epsilon_{\text{eff}}$ . In analogy with other interactions, the values of these interactions are expected to be in the range from 1 to 2 kcal/mol. Our calculations indicate that variation of  $\epsilon_2$  in this range does not change the main conclusions obtained. All the results presented below correspond to  $\epsilon_2 = 1 \text{ kcal/mol}$ . To estimate  $\epsilon_{\text{eff}}$ , we compared the measured and calculated reaction rates at  $P_{\text{NO}} = P_{\text{CO}} = 8 \text{ Torr}$  and  $T = 600 \text{ K}$ . With  $\epsilon_{\text{eff}} = 0$ , the calculated rate is much higher (two orders of magnitude) than the measured one. The rates coincide if  $z\epsilon_{\text{eff}} = 7 \text{ kcal/mol}$  (i.e.,  $\epsilon_{\text{eff}} \approx 1.2 \text{ kcal/mol}$ ). With this value of  $z\epsilon_{\text{eff}}$ , employed in the simulations, the NO dissociation rate rapidly decreases with increasing coverage. The latter is in good qualitative agreement with the UHV measurements [14b,16].

In summary, almost all the parameters used in our simulations have been obtained from UHV studies. We have deliberately avoided to introduce elementary steps or free parameters, which are not well established at UHV, because our goal was rather to reveal the shortcomings of extrapolation from UHV to high pressures, with present knowledge, than to reach a “perfect” fit of the high-pressure data.

Employing the data collected in table 1, we have analyzed the reaction kinetics over a wide range of pressures (see, e.g., fig. 1). In the UHV limit, the results of our calculations are in reasonable agreement with the experiment [17] (this part of the work will be presented in detail elsewhere [21]). In this communication, we focus our attention on the model predictions at relatively high pressures because the results obtained in this limit are most instructive from a practical point of view. In particular, comparing the dependence of the calculated and measured reaction rates on reactant pressures and temperature makes it possible to get some new insight into the reaction mechanism.

If the CO pressure is constant (e.g.,  $P_{\text{CO}} = 8 \text{ Torr}$ ,

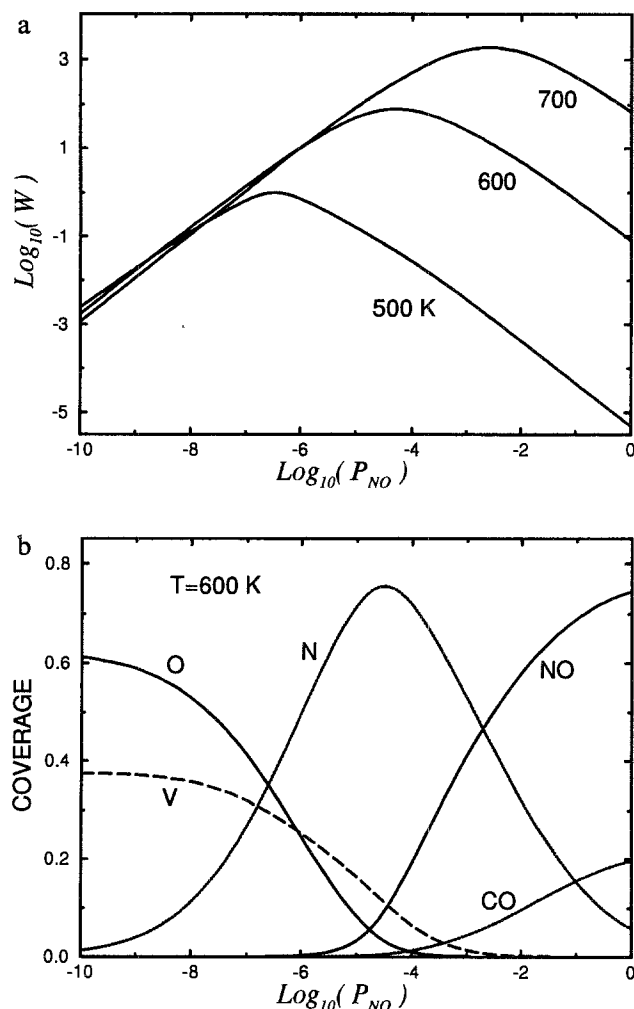


Fig. 1. Reaction rate,  $W$  ( $N_2$  molecules/(site s)), and adsorbate coverages normalized to  $\theta_s$  as a function of NO pressure,  $P_{NO}$  (bar), for  $P_{CO} = P_{NO}$  and  $T = 500, 600$  and  $700$  K. The dashed line on panel (b) shows the fraction of vacant sites.

fig. 2), the predicted dependence of the reaction rate on NO pressure is typical of Langmuir-Hinshelwood heterogeneous kinetics. First (at  $P_{NO} < 0.1$  Torr), the reaction rate increases with increasing pressure. Then, it reaches a maximum (at  $P_{NO} \approx 0.3$  Torr). Further increase in  $P_{NO}$  results in a decrease of the reaction rate. At  $P_{NO} \approx P_{CO} = 8$  Torr, the predicted reaction order with respect to NO is about  $-0.7$ . This value is in marginal agreement with the experiment which indicates that the reaction order is only slightly below zero [12].

If the NO pressure is constant (about 10 Torr), the calculated reaction rate is in fact independent of the CO pressure [21]. This prediction is in good agreement with the observed zero reaction order with respect to CO [12].

The Arrhenius curve for the reaction at  $P_{NO} = P_{CO} = 8$  Torr is shown in fig. 3. The calculated apparent activation energy, 53 kcal/mol, can be rationalized if one takes into account that the reaction is limited by NO dissociation and that NO and CO are close to the adsorption/desorption equilibrium. The value obtained is

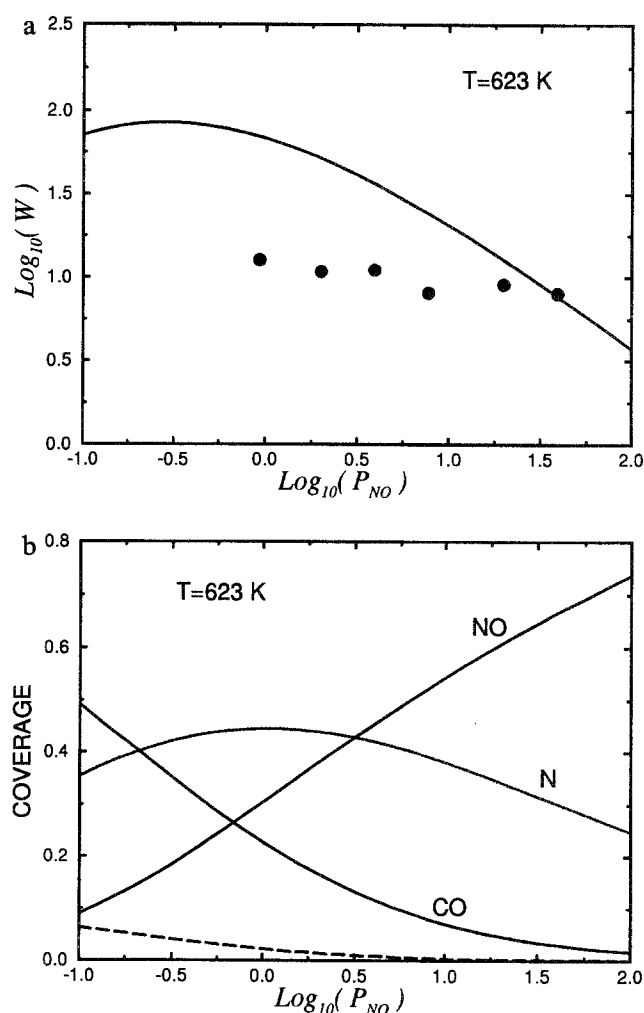


Fig. 2. Reaction rate,  $W$  ( $N_2$  molecules/(site s)), and adsorbate coverages normalized to  $\theta_s$  as a function of NO pressure,  $P_{NO}$  (Torr), for  $P_{CO} = 8$  Torr and  $T = 623$  K. The dashed line on panel (b) shows the fraction of vacant sites. Filled circles (panel (a)) indicate the reaction rate measured by Peden et al. [12].

however considerably higher than the measured one, 32 kcal/mol [12].

In summary, the high-pressure reaction kinetics, predicted by a model constructed on the basis of UHV data, is in poor agreement with the experiment. Below we consider three types of modifications of the model that can improve the agreement.

(i) Employing the reaction mechanism proposed above, it was possible to change the coverage dependence of the activation energies for some steps as follows:

(a) Near saturation, the coverage dependence of the activation energies for NO and CO desorption might be much stronger than those used in simulations. In this case, the temperature and pressure dependence of the fraction of vacant sites and accordingly of the NO dissociation rate would be weaker.

(b) One might assume that the activation energy for NO decomposition increases much more strongly with increasing N coverage than predicted by eq. (14) with

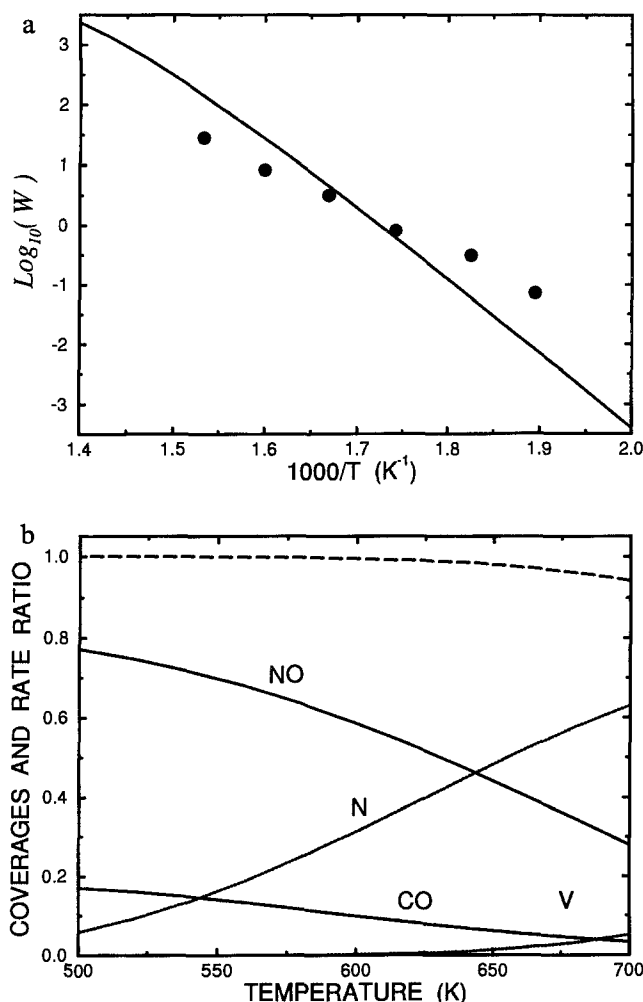


Fig. 3. Reaction rate,  $W$  ( $N_2$  molecules/(site s)), and adsorbate coverages normalized to  $\theta_s$  as a function of temperature for  $P_{CO} = P_{NO} = 8$  Torr. The curve marked by V (panel (b)) shows the fraction of vacant sites. The dashed line in panel (b) indicates the ratio of the adsorption and desorption rates for NO (for CO, the results are in fact the same). Filled circles (panel (a)) represent the reaction rate measured by Peden et al. [12].

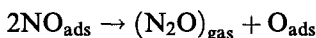
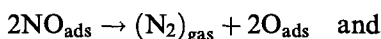
$z\epsilon_{\text{eff}} = 7$  kcal/mol. Noting that the N coverage increases with increasing temperature (fig. 3b), one would then obtain lower values of the apparent activation energy for the reaction and in addition, the predicted reaction order with respect to NO would be closer to zero. Both these effects would improve the agreement with the experiment. Physically, however, it is not quite clear why N atoms should suppress NO decomposition more strongly than NO or CO molecules do. Really, we might suspect the opposite, if for example the decrease of the NO-decomposition rate with increasing coverage is connected with steric hindrance.

(c) To reduce the apparent activation energy for the whole reaction, one might simply reduce the activation energy for NO decomposition at low coverages and simultaneously reduce the pre-exponential factor for this step (see a relevant discussion in ref. [25]). It is difficult, however, to rationalize a low value of the pre-exponential factor in the case of a uniform surface. One

possibility is that NO decomposition on Rh(111) occurs primarily on defects, e.g., steps (this mechanism seems to operate on Pd(112) [26] and Ru(0001) [27]). If the latter is the case, the defects have to be explicitly involved into the reaction scheme.

(ii) The agreement between the theory and experiment might be improved somewhat by introducing more than one type of adsorption site (the difficulties with identification of adsorption sites are discussed in ref. [16]). We do not expect however that such a modification will result in a considerable decrease of the apparent activation energy for the reaction.

(iii) At high coverages, one might have to relax the assumption that NO decomposition (step (3)) followed by  $N_2$  desorption (step (4)) is the dominant step for  $N_2$  removal, due to site blocking. Here new steps might have to be considered, e.g., direct recombination of N atoms from undissociated NO,



Clear experimental evidence for these steps is, however, lacking at present.

The results of our simulations illustrate one of the main difficulties of extrapolation of the data obtained at UHV conditions to atmospheric pressures. The problem is that the former data (e.g., the Arrhenius parameters for NO decomposition) correspond to relatively low coverages. In contrast, the adsorbed overlayer is close to saturation at high pressures. Even if the reaction mechanism is the same in both cases, the behaviour of the rate constants near saturation is not sufficiently well known and can barely be obtained from low pressure data.

Concluding this letter, we note that the understanding of the NO–CO reaction on Rh(111) is still limited and thus of considerable interest for further experimental and theoretical studies.

## Acknowledgement

This work was financially supported by the Swedish Research Council for Engineering Sciences. One of us (VPZh) is also thankful to the Swedish Institute for partial support of his stay at Chalmers University of Technology.

## References

- [1] P. Stoltze and J.K. Nørskov, Phys. Rev. Lett. 55 (1985) 2502; P. Stoltze, Phys. Scripta 36 (1987) 824; M. Bowker, I. Parker and K.C. Waugh, Appl. Catal. 14 (1985) 101; Surf. Sci. 197 (1988) L223; J.A. Dumesic and A.A. Treviño, J. Catal. 116 (1989) 119.
- [2] S.H. Oh, G.B. Fisher, J.E. Carpenter and D.W. Goodman, J. Catal. 100 (1986) 360.

- [3] B.K. Cho, J. Catal. 138 (1992) 255; 148 (1994) 697.
- [4] V.P. Zhdanov and B. Kasemo, Appl. Surf. Sci. 74 (1994) 147.
- [5] B. Hellsing, B. Kasemo and V.P. Zhdanov, J. Catal. 132 (1991) 210;  
V.P. Zhdanov and B. Kasemo, Surf. Sci. Rep. 20 (1994) 111.
- [6] C.V. Ovensen, P. Stoltze, J.K. Nørskov and C.T. Campbell, J. Catal. 134 (1992) 445.
- [7] T.S. Askgaard, J.K. Nørskov, C.V. Ovesen and P. Stoltze, J. Catal. 156 (1995) 229.
- [8] K.C. Taylor, Catal. Rev. Sci. Eng. 35 (1993) 457.
- [9] D.N. Belton and S.J. Schmieg, J. Catal. 138 (1992) 70.
- [10] D.N. Belton and S.J. Schmieg, J. Catal. 144 (1993) 9.
- [11] K.Y.S. Ng, D.N. Belton, S.J. Schmieg and G.B. Fisher, J. Catal. 146 (1994) 394.
- [12] C.H.F. Peden, D.N. Belton and S.J. Schmieg, J. Catal. 155 (1995) 204.
- [13] L. Bugyi and F. Solymosi, Surf. Sci. 258 (1991) 55.
- [14] (a) D.N. Belton, C.L. DiMaggio and K.Y.S. Ng, J. Catal. 144 (1993) 273;  
(b) D.N. Belton, C.L. DiMaggio, S.J. Schmieg and K.Y.S. Ng, J. Catal. 157 (1995) 559.
- [15] T.W. Root, L.D. Schmidt and G.B. Fisher, Surf. Sci. 134 (1983) 30.
- [16] H.J. Borg, J.F.C.-J.M. Reijerse, R.A. van Santen and J.W. Niemantsverdriet, J. Chem. Phys. 101 (1994) 10052.
- [17] S.B. Schwartz, G. Fisher and L.D. Schmidt, J. Phys. Chem. 92 (1988) 369.
- [18] C.H.F. Peden, D.W. Goodman, D.S. Blair, P.J. Berlowitz, G.B. Fisher and S.H. Oh, J. Phys. Chem. 92 (1988) 1563.
- [19] M. Shelef and G.W. Graham, Catal. Rev. Sci. Eng. 36 (1994) 433.
- [20] V.P. Zhdanov, Catal. Lett. 37 (1996) 163.
- [21] V.P. Zhdanov and B. Kasemo, to be published.
- [22] V.P. Zhdanov, Surf. Rev. Lett. (1996), in press.
- [23] V.P. Zhdanov, *Elementary Physicochemical Processes on Solid Surfaces* (Plenum, New York, 1991) ch. 4.3.
- [24] V.P. Zhdanov and B. Kasemo, J. Chem. Phys. 104 (1996) 2446.
- [25] C. Sellmer, V. Schmatloch and N. Kruse, Catal. Lett. 35 (1995) 165.
- [26] R.D. Ramsier, Q. Gao, H.N. Waltenburg and J.T. Yates Jr, J. Chem. Phys. 100 (1994) 6837.
- [27] T. Zambelli, J. Trost, J. Wintterlin and G. Ertl, Phys. Rev. Lett. 76 (1996) 795.